Geophysical Journal International

Geophys. J. Int. (2022) **228,** 2056–2060
Advance Access publication 2021 November 12
GJI Gravity, Geodesy and Tides

https://doi.org/10.1093/gji/ggab464

Accounting for GIA signal in GRACE products

Bramha Dutt Vishwakarma [1,2], Martin Horwath [3], Andreas Groh[3] and Jonathan L. Bamber[1,4]

[1]*School of Geographical Sciences, University of Bristol, Bristol BS*8 1*RL, UK. E-mail: bd.vishwakarma@bristol.ac.uk*
[2]*Interdisciplinary Centre for Water Research, Indian Institute of Science, Bangalore* 560012*, India*
[3]*Institut für Planetare Geodäsie, Technische Universität Dresden,* 01062 *Dresden, Germany*
[4]*AI4EO Future Lab, Technische Universität Munich,* 80333 *Munich, Germany*

Accepted 2021 November 10. Received 2021 November 2; in original form 2021 August 14

SUMMARY

The Gravity Recovery and Climate Experiment (GRACE) observes gravitational potential anomalies that include the effects of present-day surface mass change (PDSMC)- and glacial isostatic adjustment (GIA)-driven solid Earth mass redistribution. Therefore, GIA estimates from a forward model are commonly removed from GRACE to estimate PDSMC. There are several GIA models and to facilitate users in using a GIA model of their choice, both GRACE and GIA products are made available in terms of global gridded fields representing mass anomaly. GRACE-observed gravitational potential anomalies are represented in terms of equivalent water height (EWH) with a relation that accounts for an elastic solid Earth deformation due to PDSMC. However, for obtaining GIA EWH fields from GIA gravitational potential fields, two relations are being used: one that is similar to that being used for GRACE EWH and the other that does not include an elastic deformation effect. This leaves users with the possibility of obtaining different values for PDSMC with a given GRACE and GIA field. In this paper, we discuss the impact of this problem on regional mass change estimates and highlight the need for consistent treatment of GIA signals in GRACE observations.

Key words: Global change from geodesy; Satellite geodesy; Time variable gravity.

1 INTRODUCTION

The Gravity Recovery and Climate Experiment (GRACE) satellite mission observed mass redistribution in the Earth system at unprecedented spatiotemporal scales (Vishwakarma *et al.* 2018; Tapley *et al.* 2019). This novel observation has helped us measure ice-sheet and glacier mass change, explain sea level budget, track droughts and floods, map post-seismic response of the solid Earth after earthquakes and estimate glacial isostatic adjustment (GIA) signal (Wu *et al.* 2010; Tapley *et al.* 2019). Therefore, GRACE data have become an important tool for several disciplines of Earth sciences. One of the reasons for the popularity of GRACE is the format in which its results are disseminated. GRACE observes changes in the distance between two satellites in the same orbit, which is related to the gravitational potential field of the Earth, while the final output is, among others, available in terms of either spherical harmonic (SH) representations of the gravitational potential or gridded equivalent water height (EWH) fields representing surface mass change (Wahr *et al.* 1998). EWH is an imaginary uniform layer of water with height h over a grid cell that would result in a gravitational potential perturbation that would be observed by the GRACE satellites. Obtaining EWH from gravitational potential is an inverse problem that is solved with the help of several approximations and assumptions (Wahr *et al.* 1998). This means that EWH fields suffer from several caveats that were explained by Chao (2016), and the end user should carefully consider them before using EWH fields.

The GIA effect should be removed from GRACE fields to estimate present-day surface mass change (PDSMC), such as ice-sheet mass balance, barystatic sea level change, land water storage change and so on (Peltier 2009; Tapley *et al.* 2019). To reach a larger scientific community across disciplines and to facilitate users in choosing a GIA correction, GRACE products and various GIA model estimates are disseminated in terms of gridded EWH fields. While there is no ambiguity in converting GRACE-observed geopotential anomalies to EWH grids, two different relations have been published to convert GIA-related geopotential trends to EWH grids: one that accounts for an elastic response to EWH (Peltier 2004; Tellus 2019) and the other that does not account for an elastic response (Wu *et al.* 2010; Ivins *et al.* 2013; Caron *et al.* 2018a). Therefore, users are left with two versions of GIA EWH fields to choose from. It is very well known that the PDSMC estimates are largely affected by huge uncertainties in GIA (Sasgen *et al.* 2017; Shepherd *et al.* 2018; Willen *et al.* 2020), and an additional error due to inconsistent treatment of GIA needs to be avoided. In this

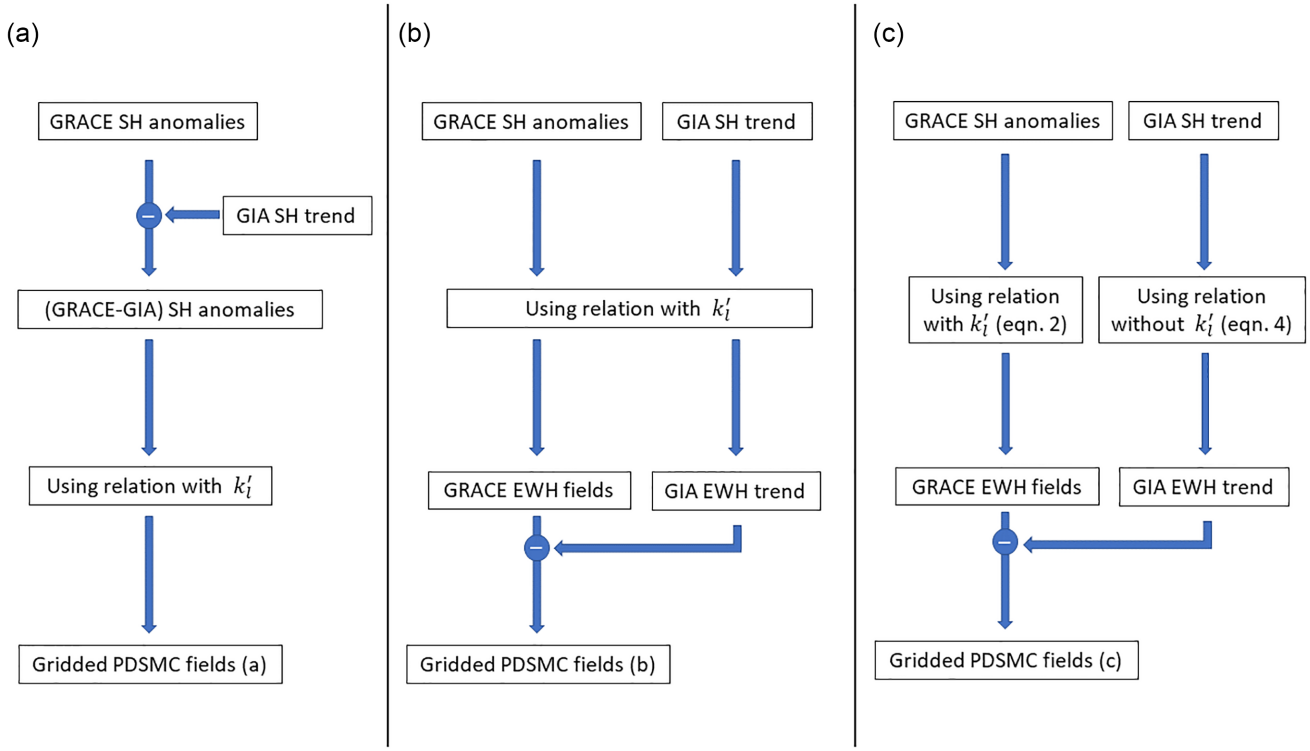

Figure 1. Various options available to users for deriving PDSMC estimates.

paper, we reiterate the relations that are being used to obtain gridded GIA products, discuss all the possible PDSMC estimates that can be obtained from a given GRACE product and a GIA model, and finally comment on the accuracy of each estimate of PDSMC and the need for consistency.

2 EWH FIELDS FROM GEOPOTENTIAL

GRACE level 2 products include sets of SH coefficients representing monthly averages of the gravitational field of the Earth. Subtracting a mean gravitational field from these SH coefficients gives us residual SH coefficients that are noisy and filtering is one way to suppress the noise (Wahr *et al.* 1998; Swenson & Wahr 2006; Vishwakarma *et al.* 2017). Following Wahr *et al.* (1998), we can convert these SH coefficients to EWH fields. The filtered residual SH coefficients, denoted by ΔC_{lm} and ΔS_{lm}, are related to surface density change $\Delta\sigma(\theta, \lambda)$ assuming that the mass redistribution takes place within a thin layer near the Earth's surface (Wahr *et al.* 1998),

$$\Delta\sigma(\theta,\lambda) = \frac{a\rho_{\rm avg}}{3}\sum_{l=0}^{L_{\rm max}}\sum_{m=0}^{l}\bar{P}_{lm}(\cos\theta)\frac{2l+1}{1+k_l'} \times [\Delta C_{lm}\ \cos m\lambda + \Delta S_{lm}\ \sin m\lambda], \quad (1)$$

where $\rho_{\rm avg}$ is the average density of the Earth (5517 kg m^{-3}), a is the mean radius of the Earth, θ is the co-latitude, λ is the longitude and $\bar{P}_{lm}$ are the fully normalized Legendre functions for degree l and order m. Eq. (1) accounts for the solid Earth's elastic deformation induced by a surface mass change. The gravity field effect of this elastic deformation is represented by inclusion of the potential load Love numbers k_l' (Farrell 1972; Wahr *et al.* 1998; van Dam *et al.* 2007). $\Delta\sigma(\theta, \lambda)$ can be written as a product of density of water $\rho_{\rm water}$ and EWH, resulting in

$$\mathrm{EWH}(\theta,\lambda) = \frac{a\rho_{\rm avg}}{3\rho_{\rm water}}\sum_{l,m}\bar{P}_{lm}(\cos\theta)\frac{2l+1}{1+k_l'} \times [\Delta C_{lm}\ \cos m\lambda + \Delta S_{lm}\ \sin m\lambda]. \quad (2)$$

Since GIA-related solid Earth mass redistribution is also recorded by GRACE, it is required to remove GIA predictions from a forward model to obtain estimates of PDSMC (Wahr *et al.* 1998; Peltier 2009). GIA model outputs are available in terms of the rate of change of the gravitational potential (level 2 SH products), which can then be converted to EWH (level 3 gridded products) providing users with an option to remove GIA from GRACE at either level 2 or level 3. One way of converting modelled GIA-induced geopotential trends to EWH is to use a relation analogous to eq. (2):

$$\mathrm{EWH}^{b}_{\rm GIA}(\theta,\lambda) = \frac{a\rho_{\rm avg}}{3\rho_{\rm water}}\sum_{l,m}\bar{P}_{lm}(\cos\theta)\frac{2l+1}{1+k_l'} \times [\Delta C^{\rm GIA}_{lm}\ \cos m\lambda + \Delta S^{\rm GIA}_{lm}\ \sin m\lambda], \quad (3)$$

wherein the GIA SH coefficients are denoted by $\Delta C^{\rm GIA}_{lm}$ and $\Delta S^{\rm GIA}_{lm}$. This expression describes a hypothetical surface mass redistribution on an elastic Earth that would cause the same gravity anomaly as the modelled GIA. This relation is favoured in Peltier (2009) and is more commonly used. Another way of converting modelled GIA-induced geopotential trend to EWH is to exclude k_l':

$$\mathrm{EWH}^{c}_{\rm GIA}(\theta,\lambda) = \frac{a\rho_{\rm avg}}{3\rho_{\rm water}}\sum_{l,m}\bar{P}_{lm}(\cos\theta)(2l+1) \times [\Delta C^{\rm GIA}_{lm}\ \cos m\lambda + \Delta S^{\rm GIA}_{lm}\ \sin m\lambda]. \quad (4)$$

In this case, EWH is a hypothetical surface mass redistribution on a rigid Earth that would cause the same gravity anomaly as the

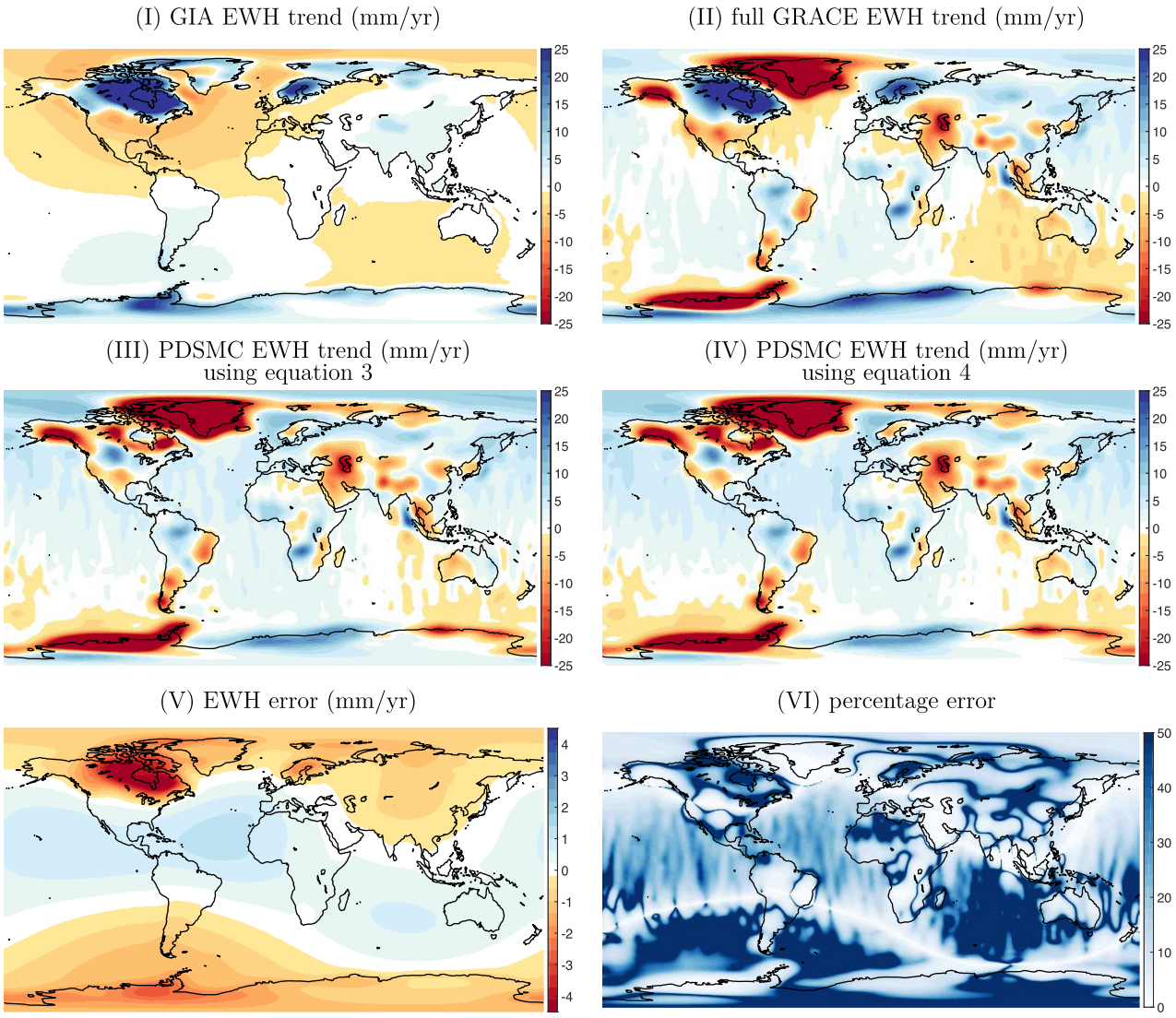

Figure 2. Panel (I) shows the GIA EWH in mm yr^{-1} from the Caron *et al.* (2018a) GIA model (using eq. 3); panel (II) shows GRACE total mass change trends in mm yr^{-1} of EWH; panel (III) shows GRACE PDSMC trends in mm yr^{-1} of EWH derived using option (b); panel (IV) shows GRACE PDSMC trends in mm yr^{-1} of EWH derived using option (c); panel (V) shows the error obtained by subtracting panel (III) from panel (IV); and panel (VI) shows the percentage error.

modelled GIA. This relation was used by Wu *et al.* (2010, 2012), Ivins *et al.* (2013) and Caron *et al.* (2018a).

3 VARIOUS POSSIBLE PDSMC ESTIMATES FROM A GIVEN GRACE AND GIA FIELD

In Fig. 1, we show three possible ways for obtaining PDSMC estimates. In option (a) (Fig. 1a), the GIA SH trend is first subtracted from GRACE SH anomalies, and then using eq. (2) PDSMC estimates are obtained (Wahr *et al.* 1998; Peltier 2009). However, this requires level 2 processing expertise at the user end and provides no flexibility to a level 3 user. Therefore, options (b) and (c) are opted by level 3 users, where they download GRACE level 3 products (obtained using eq. 2), and then remove GIA EWH fields of their choice. These GIA EWH fields may be obtained by either eq. (3) or eq. (4). In option (b), eq. (2) is used on GRACE level 2 data (GIA + PDSMC), which is equivalent to applying eq. (2) consistently to both PDSMC and GIA signals. Using the same equation to obtain GIA EWH fields (*cf.* eq. 3) and then removing it from GRACE EWH fields is equivalent to removing GIA at level 2. Hence, PDSMC estimates from option (b) are equivalent to option (a), and are correct. On the other hand, in option (c), eq. (2) is used on GRACE (GIA + PDSMC) but a slightly different relation (eq. 4) is used for obtaining GIA EWH fields, which leads to an error in the PDSMC EWH fields:

$$\text{error}_c(\theta,\lambda) = \frac{a\rho_{\text{avg}}}{3\rho_{\text{water}}}\sum_{l,m}\bar{P}_{lm}(\cos\theta)\frac{(2l+1)k_l'}{1+k_l'} \times [\Delta C_{lm}^{\text{GIA}}\cos m\lambda + \Delta S_{lm}^{\text{GIA}}\sin m\lambda]. \quad (5)$$

Since the full GIA signal is mass conserving ($C_{00}^{\text{GIA}} = 0$), the global average of this error is zero. However, the error has significant implications for regional studies. This is further discussed in Section 4.

Table 1. Error due to a GIA correction inconsistency (5) on estimates of regional mass change rates. The GIA model by Caron *et al.* (2018a) is used here.

Region	Error	Nature of error	PDSMC estimates from literature
Oceans	$+0.1$ mm yr^{-1}	Underestimated	$+1.63 \pm 0.1$ mm yr^{-1} (Vishwakarma *et al.* 2020)
East Antarctica	-15.3 Gt yr^{-1}	Overestimated	$+15 \pm 41$ Gt yr^{-1} (Shepherd *et al.* 2018)
West Antarctica and peninsula	-2.0 Gt yr^{-1}	Overestimated	-120 ± 30 Gt yr^{-1} (Shepherd *et al.* 2018)
Antarctic Ice Sheet	-17.3 Gt yr^{-1}	Overestimated	-105 ± 51 Gt yr^{-1} (Shepherd *et al.* 2018)
Greenland Ice Sheet	-1.2 Gt yr^{-1}	Overestimated	-248 ± 18 Gt yr^{-1} (Shepherd *et al.* 2020)

4 ERRORS DUE TO INCONSISTENT GIA CORRECTION

To illustrate the error due to an inconsistent treatment of GIA, we used the ITSG-Grace2018 level 2 SH product from the Institute of Geodesy, Graz (Mayer-Gürr *et al.* 2018; Kvas *et al.* 2019), for a period from January 2003 to December 2015 inclusive. The GIA model outputs are taken from Caron *et al.* (2018a). They are given in terms of the rate of change in gravitational potential and we converted them to EWH using either eq. (3) or eq. (4). It can be shown that the GIA EWH fields provided by Caron *et al.* (2018a) on https://vesl.jpl.nasa.gov/solid-earth/gia/ can be reproduced when using eq. (4) (Caron *et al.* 2018b). The recommended post-processing steps for GRACE data were followed: replacing the C_{20} and degree 1 coefficients (Swenson *et al.* 2007; Cheng *et al.* 2013), subtracting a mean static gravity field (computed from monthly SH coefficients between January 2004 and December 2009) to obtain residual SH coefficients and filtering with a Gaussian filter of half-width radius of 400 km (Wahr *et al.* 1998). The residual SH coefficient time-series was decomposed into an intercept, a linear trend, a semi-annual signal and an annual signal using least-squares regression (Vishwakarma *et al.* 2020). Here, we use linear trends from GRACE and the GIA model. The difference between the PDSMC rates obtained from options (b) and (c) is not negligible and is shown in panel V of Fig. 2. Panel (I) shows the GIA EWH trends obtained using eq. (3), panel (II) shows GRACE total mass change trends, panel (III) shows the PDSMC from option (b), panel (IV) shows the PDSMC from option (c) and the percentage error $E_{\%}$ is shown in panel (VI). The percentage error is computed as

$$|E_{\%}|(\theta, \lambda) = \frac{\mathrm{EWH}_{\mathrm{error}}(\theta, \lambda)}{\mathrm{EWH}_{\mathrm{correct}}(\theta, \lambda)} \times 100. \quad (6)$$

We also compute area weighted averages of the error for five regions: (i) oceans, (ii) East Antarctica, (iii) West Antarctica and the Antarctic Peninsula, (iv) Antarctic Ice Sheet, (v) Greenland Ice Sheet and (vi) continents, except Antarctica and Greenland. The results are shown in Table 1. We conclude that due to such an error, the Antarctic ice mass loss rate would be overestimated by $\approx$18 per cent and the ocean mass increase rate would be underestimated by $\approx$6 per cent. This further demonstrates the importance of removing the GIA signal consistently. The error here is a function of the GIA model only, which is clear from eq. (5). Therefore, these numbers will change if we replace the Caron *et al.* (2018a) GIA model used here by a different GIA model.

4.1 Ensuring consistent treatment of GIA

Options (a) and (b) ensure a consistent treatment of GIA and provide equivalent results. Option (a) is the simplest by concept, as it avoids the concept of EWH GIA grids, which might be subject to misinterpretation. Option (b) offers flexibility to level 3 users for choosing a GIA model. Option (c) leads to an error demonstrated in eq. (5) and illustrated in Fig. 2. An additional option arises if users download a gridded PDSMC field that is already corrected for GIA and then want to apply a different GIA correction. These gridded fields could be level 3 GRACE products or the mascons, which are readily available from various data centres. In this case, users need to add back the previously removed GIA field and remove a GIA grid of their choice. Here, users should ensure consistency. Any provision of GIA EWH fields should include information on the relation used (eq. 3 or eq. 4).

5 CONCLUSIONS

Subtracting the GIA signal is essential to accurately determine the PDSMC from GRACE data. The interdisciplinary appeal of the mission motivated research institutions and data centres to provide users with easy to use data sets, which resulted in the availability of various gridded GRACE products and GIA models. Many studies remove gridded GIA of their choice from GRACE to obtain PDSMC fields. Two relations are being used to obtain GIA EWH fields from SH representations of GIA, leading to two different GIA EWH products. In this contribution, we described various combinations of GRACE and GIA to obtain three PDSMC estimates and discuss which one is correct. Using GRACE products from TU Graz and GIA estimates from Caron *et al.* (2018a), we show that an inconsistent treatment of GIA can lead to an overestimation of ice-sheet mass losses (-17.3 Gt yr^{-1} over Antarctica) and an underestimation of ocean mass change ($+0.1$ mm yr^{-1}). Similar errors will occur when replacing GIA solution in level 3 GRACE products, including mascons. Therefore, users should carefully account for GIA in GRACE products.

ACKNOWLEDGEMENTS

A number of colleagues have helped with suggestions for the improvement of this material and we would particularly like to thank Erik Ivins and Lambert Caron from JPL NASA, Ricardo Riva from TU Delft and three anonymous referees.

BDV was supported by the Marie Skłodowska-Curie Individual Fellowship (MSCA-IF) under grant agreement number 841407 (CLOSeR). AG was supported by ESA through the Climate Change Initiative (CCI) projects Sea-level Budget Closure CCI (contract number 4000119910/17/I-NB), Antarctic Ice Sheet CCI+ (contract number 4000126813/19/I-NB) and Greenland Ice Sheet CCI+ (contract number 4000126523/19/I-NB). JLB was supported by European Research Council (ERC) under the European Union's Horizon 2020 - Research and Innovation Framework Programme under grant agreement number 694188, the GlobalMass project

(globalmass.eu). JLB was additionally supported through a Leverhulme Trust Fellowship (RF-2016-718) and a Royal Society Wolfson Research Merit Award https://royalsociety.org/grants-schemes-awards/grants/wolfson-research-merit/.

DATA AVAILABILITY

The authors are grateful for the open availability of observational data sets. The source of each data set is cited in the main text. GRACE data and the low degree coefficient time-series for GRACE are available at https://www.tugraz.at/institute/ifg/downloads/gravity-field-models/itsg-grace2018/ and https://podaac.jpl.nasa.gov/. GIA data are available at https://vesl.jpl.nasa.gov/solid-earth/gia/, kindly provided by Caron *et al.* (2018a). The MATLAB scripts used to process GRACE spherical harmonic coefficients can be downloaded from https://www.gis.uni-stuttgart.de/en/research/downloads/.

REFERENCES

Caron, L., Ivins, E.R., Larour, E., Adhikari, S., Nilsson, J. & Blewitt, G., 2018a. GIA model statistics for GRACE hydrology, cryosphere, and ocean science, *Geophys. Res. Lett.,* **45**(5), 2203–2212.

Caron, L., Ivins, E.R., Larour, E., Adhikari, S., Nilsson, J. & Blewitt, G., 2018b. 'Glacial isostatic adjustment simulations'. Virtual Earth System Laboratory. Available at: https://vesl.jpl.nasa.gov/solid-earth/gia/ (accessed 15 Dec. 2019).

Chao, B., 2016. Caveats on the equivalent water thickness and surface mascon solutions derived from the GRACE satellite-observed time-variable gravity, *J. Geod.,* **90**(9), 807–813.

Cheng, M., Tapley, B.D. & Ries, J.C., 2013. Deceleration in the Earth's oblateness, *J. geophys. Res.,* **118**(2), 740–747.

Farrell, W.E., 1972. Deformation of the Earth by surface loads, *Rev. Geophys.,* **10**(3), 761–797.

Ivins, E.R., James, T.S., Wahr, J., O.Schrama E.J., Landerer, F.W. & Simon, K.M., 2013. Antarctic contribution to sea level rise observed by GRACE with improved GIA correction, *J. geophys. Res.,* **118**(6), 3126–3141.

Kvas, A., Behzadpour, S., Ellmer, M., Klinger, B., Strasser, S., Zehentner, N. & Mayer-Gürr, T., 2019. ITSG-Grace2018: overview and evaluation of a new GRACE-only gravity field time series, *J. geophys. Res.,* **124**(8), 9332–9344.

Mayer-Gürr, T., Behzadpour, S., Ellmer, M., Kvas, A., Klinger, B. & Zehentner, N., 2018. 'ITSG-Grace2018: monthly, daily and static gravity field solutions from GRACE'. GFZ Data Services. Available at: https://www.tugraz.at/institute/ifg/downloads/gravity-field-models/itsg-grace2018/ (accessed 20 Jan. 2018).

Peltier, W., 2004. Global glacial isostasy and the surface of the ice-age Earth: the ICE-5G (VM2) model and GRACE, *Annu. Rev. Earth Planet. Sci.,* **32,** 111–149.

Peltier, W., 2009. Closure of the budget of global sea level rise over the GRACE era: the importance and magnitudes of the required corrections for global glacial isostatic adjustment, *Quat. Sci. Rev.,* **28**(17), 1658–1674.

Sasgen, I. *et al.*, 2017. Joint inversion estimate of regional glacial isostatic adjustment in Antarctica considering a lateral varying Earth structure (ESA STSE Project REGINA), *Geophys. J. Int.,* **211**(3), 1534–1553.

Shepherd, A. *et al.*, 2018. Mass balance of the Antarctic Ice Sheet from 1992 to 2017, *Nature,* **558,** 219–222.

Shepherd, A. *et al.*, 2020. Mass balance of the Greenland Ice Sheet from 1992 to 2018, *Nature,* **579**(7798), 233–239.

Swenson, S. & Wahr, J., 2006. Post-processing removal of correlated errors in GRACE data, *Geophys. Res. Lett.,* **33**(8), L08402, doi:10.1029/2005GL025285.

Swenson, S., Chamber, D. & Wahr, J., 2007. Estimating geocenter variations from a combination of grace and ocean model output, *J. geophys. Res.,* **113,** B08410, doi:10.1029/2007JB005338.

Tapley, B.D. *et al.*, 2019. Contributions of GRACE to understanding climate change, *Nat. Clim. Change,* **9,** 358–369.

Tellus, 2019. TELLUS_GIA_1-Deg_v1.0. Ver. 1.0. PO.DAAC, CA, USA. Dataset, PO.DACC Data Repository.

van Dam, T., Wahr, J. & Lavallée, D., 2007. A comparison of annual vertical crustal displacements from GPS and Gravity Recovery and Climate Experiment (GRACE) over Europe, *J. geophys. Res.,* **112**(B3), B03404, doi:10.1029/2006JB004335.

Vishwakarma, B., Royston, S., Riva, R., Westaway, R. & Bamber, J., 2020. Sea level budgets should account for ocean bottom deformation, *Geophys. Res. Lett.,* **47**(3), e2019GL086492.

Vishwakarma, B.D., Horwath, M., Devaraju, B., Groh, A. & Sneeuw, N., 2017. A data-driven approach for repairing the hydrological catchment signal damage due to filtering of GRACE products, *Water Resour. Res.,* **53**(11), 9824–9844.

Vishwakarma, B.D., Devaraju, B. & Sneeuw, N., 2018. What is the spatial resolution of grace satellite products for hydrology? *Remote Sens.,* **10**(852), doi:10.3390/rs10060852.

Wahr, J., Molenaar, M. & Bryan, F., 1998. Time variability of the Earth's gravity field: hydrological and oceanic effects and their possible detection using GRACE, *J. geophys. Res.,* **103**(B12), 30 205–30 229.

Willen, M.O., Horwath, M., Schröder, L., Groh, A., Ligtenberg, S.R., Kuipers Munneke, P. & Van Den Broeke, M.R., 2020. Sensitivity of inverse glacial isostatic adjustment estimates over Antarctica, *Cryosphere,* **14**(1), 349–366.

Wu, X. *et al.*, 2010. Simultaneous estimation of global present-day water transport and glacial isostatic adjustment, *Nat. Geosci.,* **3**(9), 642–646.

Wu, X., Ray, J. & van Dam, T., 2012. Geocenter motion and its geodetic and geophysical implications, *J. Geodyn.,* **58,** 44–61.